

A Probabilistic Feature Fusion for Building Detection in Satellite Images

Dimitrios Konstantinidis¹, Tania Stathaki¹, Vasileios Argyriou² and Nikos Grammalidis³

¹*Communications and Signal Processing, Imperial College London, London, U.K.*

²*Computing and Information Systems, Kingston University, London, U.K.*

³*CERTH-ITI, Thessaloniki, Greece*

Keywords: Building Detection, Satellite Images, HOG, NDVI, FAST Algorithm, Probabilistic Fusion.

Abstract: Building segmentation from 2D images can be a very challenging task due to the variety of objects that appear in an urban environment. Many algorithms that attempt to automatically extract buildings from satellite images face serious problems and limitations. In this paper, we address some of these problems by applying a novel approach that is based on the fusion of Histogram of Oriented Gradients (HOG), Normalized Difference Vegetation Index (NDVI) and Features from Accelerated Segment Test (FAST) features. We will demonstrate that by taking advantage of the multi-spectral nature of a satellite image and by employing a probabilistic fusion of the aforementioned features, we manage to create a novel methodology that increases the performance of a building detector compared to other state-of-the-art methods.

1 INTRODUCTION

Building detection is considered an important task for several applications, such as city mapping and urban planning. Cadastral offices can use such information to prevent illegal building activity or track changes in an urban environment that can occur either naturally with the construction/demolition of buildings or by the force of nature. Another application is the analysis and assessment of the impact of fire, flood and natural disasters on an urban environment, which can assist municipalities on taking necessary measures and precautions to minimize consequences and save human lives in the future. Although building detection can be achieved manually by human experts, the speed with which modern cities change, makes the development of automatic building detection algorithms imperative. However, building detection can be a challenging task even for state-of-the-art algorithms, since buildings appear in various shapes and colors, they can be affected by weather conditions and satellite resolution and they can partially be occluded by other buildings or tall trees.

Building detection algorithms can be classified based on the dimensionality and processing method of the available data. The existence of 3D data can give rise to 3D building detection algorithms, while images allow the development of 2D algorithms. 2D algorithms can be further split to those that deal with

the task of building detection on the pixel level by employing image segmentation techniques and those that handle buildings as objects and perform model-based techniques. The proposed algorithm can be categorized as a model-based technique. It extracts three types of features from an image and classifies image blocks to those that describe a building and those that do not.

This work makes two new significant contributions to the problem of building detection. Firstly, it exploits multi-modal data as it takes advantage of all the available channels of a satellite image. Moreover, we propose the use of a novel probabilistic framework to fuse the different types of features. As we will demonstrate, these novelties can give a boost to our algorithm's performance in the building detection task.

The rest of the paper is organized as follows. In Section 2 we provide a review on state-of-the-art building detection algorithms, while in Section 3 we describe our proposed methodology. In Section 4 we present the datasets used and the experimental results obtained. Finally, conclusions are drawn in section 5.

2 RELATED WORK

Building extraction methodologies can be classified in two major categories, based on the dimensional-

ity of the data they process. The first category consists of algorithms that process 3D data, in the form of LiDAR point clouds and Digital Surface Models (DSMs) that can describe the height of a terrain. In (Hu et al., 2004), 3D planes were identified and matched to possible building rooftops, while in (Karantzalos and Paragios, 2010), 3D templates were utilized as a means to identify building shapes. Unfortunately, 3D models can be quite inaccurate due to sensor limitations and introduce significant errors to the building detection task.

In the second category of building detection methods, there are algorithms that process 2D images either on the pixel or model/object level. Caselles et al. was the first to introduce geodesic active contours as a means to segment an object of interest from an image (Caselles et al., 1995). His work inspired others to detect buildings by developing a circular cast algorithm to find appropriate initialization contours (Theng, 2006) or by constructing a suitable energy function to be used on a level-set segmentation algorithm (Karantzalos and Argyias, 2009). Nevertheless, it is hard to construct an energy function that can characterize every building in an image, due to the variety in the appearance and shape of buildings. A spatial k-means clustering algorithm was developed in (Li et al., 2007) for multi-spectral image segmentation, while super-pixels, i.e. the smallest clusters of pixels an image can be split, were used for building detection in (Kluckner and Bischof, 2010). However, the resulting clusters cannot easily be associated with buildings due to their irregular shapes.

Model-based algorithms consider buildings as objects and attempt to extract them by finding distinctive features. In (Haverkamp, 2004), graph theory is utilized to merge lines into meaningful shapes, while in (Woo et al., 2008), the authors developed a method to label and group corners so as to extract buildings. Nonetheless, noise and aliasing effects can pose problems to line and corner extraction methods. Templates, which are parameterized shapes, are employed as another way to solve the problem of building detection. 2D deformable templates and roof topology graphs were used for building detection in (Vinson et al., 2001) and (Verma et al., 2006) respectively. However, creating a template for every possible building shape that can exist in an urban environment seems impossible, so one has to make certain assumptions about the shape of the extracted buildings.

Building extraction has also been achieved by fuzzy logic and probabilistic theory. Fuzzy logic was employed on the spectral and spatial properties of pixels in (Shackelford and Davis, 2003). Markov

Random Fields (MRFs) were used as an alternative technique to separate buildings from background in a probabilistic framework (Chai et al., 2012). Finally, many techniques take advantage of the multi-spectral nature of images, and more specifically the NDVI index to separate man-made objects from vegetation (Singh et al., 2012). Shadow detection has also been incorporated in several methodologies, as a way to denote the existence of nearby tall structures, which can be candidate buildings (Benarchid et al., 2013).

Our technique can be classified as a model-based approach. We employ HOG descriptors as core features to describe buildings. A Support Vector Machine (SVM) classifier is used to discriminate between building and non-building image patches and NDVI and FAST features are computed for the identified building patches to enhance the classification performance. Our strategy overcomes some of the inherent disadvantages of other techniques. Images are easier to acquire and often yield a more accurate representation of the urban environment than 3D models. What is more, the parameters of the HOG algorithm can be tuned to work well with several images, without suffering from huge performance degradation. Finally, a HOG algorithm is robust to shape variations and can detect a variety of shapes, given that it is trained with a representative set of possible building shapes. As we will demonstrate, our proposed methodology performs better than other state-of-the-art algorithms that employ HOG features (Ilsever and Unsalan, 2013) or fuse multiple features (Sirmacek and Unsalan, 2011).

3 METHODOLOGY

In this paper, we assume that all input images are already orthorectified, which means that distortions caused from the sensor and the earth's terrain have been geometrically removed before we apply any methodology. Our approach takes an image as input and extracts HOG, NDVI and FAST features. Afterwards, it employs a Bayesian method to fuse these features and outputs a set of image regions that contain buildings.

One of the first problems that needs to be addressed when dealing with multi-spectral images is the resolution of the satellite data. A satellite can produce panchromatic images of much higher resolution than the resolution of multi-spectral images. To take advantage of the higher resolution of the panchromatic image, a procedure, known as multi-spectral band sharpening is employed. The goal is to fuse the two types of images in order to create a multi-spectral

image with the same resolution as the panchromatic image. Such a sharpened multi-spectral image can significantly enhance the accuracy of a building detection algorithm. Vrabel tested various sharpening algorithms to find out that the CN algorithm performs the best (Vrabel, 2000). According to the CN algorithm (Hallada and Cox, 1983), if MS_i is the i^{th} low-resolution multi-spectral band and PAN is the panchromatic band, then the following equation produces the i^{th} high-resolution color normalized multi-spectral band CN_i

$$CN_i = \frac{(MS_i + 1.0) * (PAN + 1.0) * 3.0}{\sum_i MS_i + 3.0} - 1.0 \quad (1)$$

The HOG algorithm was initially introduced as a means to detect pedestrians in an image (Dalal and Triggs, 2005). A HOG descriptor is computed in an image region that is further divided into subregions, which are called cells. In each cell, a 1D histogram of the orientations of the gradients of the pixels present inside the cell is computed. By tuning the parameters that affect the creation of the histograms, a feature can be developed that can differentiate image regions that contain buildings from those that do not. Our methodology, illustrated in figure 1, follows the standard approach for implementing a HOG algorithm, suggested in (Dalal and Triggs, 2005) and it can be split in two phases, i.e. a training and a testing phase.

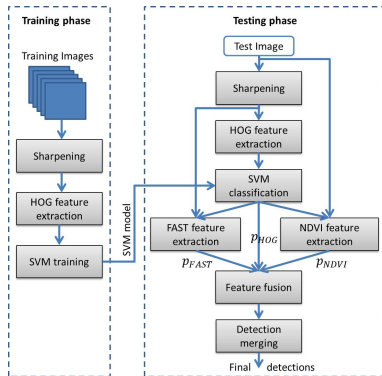


Figure 1: Our building detection implementation.

In the training phase, manually labeled images are employed and HOG descriptors for the two classes are extracted. Every image is preprocessed before the gradient computation. All pixels are initially divided with the maximum discretization value, so that they are in the range $[0,1]$ and then a sharpening filter is applied. A sharpened image is the product of the subtraction of the initial image with the same image convolved with a Gaussian filter. The purpose of the sharpening procedure is the enhancement of the

edges of an image so that buildings can become more distinguishable in an urban environment.

After preprocessing, signed gradients are computed by employing the Scharr operator separately to each multi-spectral image channel. In each cell, the computed gradients are used to cast votes into histogram bins, weighted by their magnitude. What is more, gradient magnitude is trilinearly interpolated in the neighboring cells and bins to increase the robustness of the HOG detector in slight rotations or translations of the object of interest (Dalal, 2006). A single block with a rectangular kernel is employed for the HOG descriptor extraction in an image region. The computed histograms, one for each channel of a multi-spectral image, are concatenated into a single histogram/descriptor. The HOG descriptors remain unnormalised, since such a strategy produces better results than any normalization schemes (see Section 4.2). The entire HOG feature extraction procedure is illustrated in figure 2.

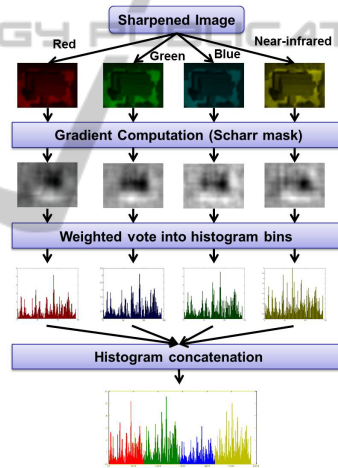


Figure 2: HOG feature extraction procedure.

The extracted HOG descriptors are then introduced to a SVM classifier with a Radial Basis Function (RBF) kernel, since such a classifier is considered suitable for binary classification problems. A SVM model is trained and is used for classification in the testing phase.

In the testing phase, each test image is split in overlapping regions of multiple sizes (scales) and a HOG descriptor is extracted for each image region. Then, the HOG descriptors are classified to the building and non-building classes, using the SVM model that was previously trained. The scores x of the SVM classifier are transformed into probabilities p_{HOG} using the sigmoid function

$$p_{HOG} = \frac{1}{1 + e^{Ax+B}} \quad (2)$$

The constant terms A and B are determined by minimizing the negative log likelihood of the training data $\min(-\sum_i(t_i * \log(p_{HOG_i}) + (1-t_i) * \log(1-p_{HOG_i})))$, where t_i is equal to 0 for negative samples and 1 for positive samples (Platt, 1999). An initial set of candidate building regions is formed by keeping only the image regions that are classified in the building class by the SVM model (i.e. SVM score x higher than 0), since the separating hyperplane is found to give the best discriminative power to our algorithm. Afterwards, the NDVI mask and FAST features are computed for these image regions. The goal is to reduce the number of false alarms that the HOG algorithm creates.

The NDVI is a well-known index that can distinguish vegetated from non-vegetated areas, since vegetation tend to produce higher values for this index than man-made structures. NDVI is computed using the near-infrared and red channels as shown below, where ρ_{NIR} and ρ_R are the near-infrared and red channels respectively.

$$NDVI = \frac{\rho_{NIR} - \rho_R}{\rho_{NIR} + \rho_R} \quad (3)$$

A threshold is automatically chosen using the Otsu's method and therefore, a binary NDVI mask can be formed to identify vegetation pixels in an image region. A probability p_{NDVI} is then computed for each region and is defined as the number of pixels in the region that are not identified as vegetation, divided by the total number of pixels in the region.

Buildings, due to their rectangular shape, usually have strong corners, which is an important cue for building segmentation. FAST algorithm is a robust corner detector, which provides a set of corner features (pixels) along with a corresponding score (i.e. intensity difference to their neighboring pixels) (Rosten and Drummond, 2006). In this paper, we compute FAST features for each sharpened channel of a multi-spectral image. If two or more features are identified in the same position(pixel), the one with the largest score is preserved.

For each candidate building region, a probability p_{FAST} is computed based on the FAST features by employing the following strategy, which is based on the notion that building corners typically point towards the center of the building, as opposed to irrelevant corners. For every feature F_i , a line L_i is defined, passing through the feature and having the orientation of the image gradient at F_i . Then, a new feature F'_i is computed as the point in L_i closest to the center of the candidate building region. For every feature F'_i , a 2D Gaussian distribution having as peak the score of F_i is defined. A sum of these distributions is computed for every pixel in a candidate building region k and the

maximum value V_k is identified, which indicates the strength of the corners in the region. The probability p_{FAST} for each region k is equal to the value V_k divided by the maximum value $\max_k(V_k)$ among all the candidate regions, assuming that the region with the highest value represents a true building.

Afterwards, the three probabilities are fused using the Bayesian method shown in equation (4) to form an overall probability that a candidate region corresponds to a building.

$$p(B|O) = \frac{p(B,O)}{p(O)} = \frac{p_{HOG} * p_{NDVI} * p_{FAST}}{\mathbf{Z}} \quad (4)$$

In equation (4), the posterior probability $p(B|O)$ of a region describing a building given the observations depends on the joint probability $p(B,O)$, which, assuming the independency of the observations, is equal to the product of probabilities p_{HOG} , p_{FAST} and p_{NDVI} . The normalization term \mathbf{Z} which equals to $p_{HOG} * p_{NDVI} * p_{FAST} + (1 - p_{HOG}) * (1 - p_{NDVI}) * (1 - p_{FAST})$ ensures that the probabilities of building and non-building add up to unity.

We accept as candidate building regions only those with a posterior probability equal or higher than 0.5. However, the HOG algorithm produces overlapping building candidate regions, hence a detection merging procedure is required. For this reason, a mean-shift algorithm (Dalal, 2006) is employed to reduce the number of detected regions. More specifically, the regions can be considered as points (x,y,z) in the 3D space weighted by their posterior probability $p(B|O)$, where x and y are the coordinates of the center of the region and z is the logarithm of the scale where the region was detected (Dalal, 2006). A set of uncertainties that describe how far points can be in order to be merged were also defined.

However, there may still be overlapping regions that cannot be merged because the selected uncertainties may not sufficiently describe the distribution of regions. To cope with this problem, we developed a rectangle grouping algorithm that detects overlapping rectangles (regions). Two rectangles are considered overlapping, if at least half the area of one rectangle is enclosed within the other rectangle. In the first phase, the algorithm discards large rectangles that overlap with two or more smaller rectangles that do not overlap with each other. Such rectangles cannot be considered as appropriate building regions because they usually contain two or more buildings that are described by the enclosed regions. In the second phase, the remaining pairs of overlapping regions are compared and the region with the highest posterior probability $p(B|O)$ is preserved, while the other is discarded. The remaining regions define the final output of our methodology.

4 EXPERIMENTS AND RESULTS

In this section, we describe our dataset, present the experiments for the optimal parameter configuration and demonstrate the performance of our method on a test set. Finally, we compare our algorithm with another HOG implementation that was developed in (Ilsever and Unsalan, 2013) and another state-of-the-art methodology that fuses various corner features as described in (Sirmacek and Unsalan, 2011).

4.1 Dataset

Our training dataset consists of 700 positive and 1000 negative manually segmented and labeled QuickBird images. The positive samples contain buildings in arbitrary orientations in order to increase the robustness of the HOG detector in the building orientation. To further increase the accuracy of the classifier, 400 hard negatives are obtained by executing the HOG algorithm on QuickBird images with no buildings and are used to re-train the SVM classifier.

Our test set consists of 29 images depicting a suburban area of Athens, Greece, along with their ground truth data of building locations. All the images depict 6 different areas that are captured on 5 different time intervals each and more specifically in years 2006, 2007, 2009 for the QuickBird satellite and 2010, 2011 for the WorldView 2 satellite.

The parameter selection for the HOG implementation is based on a validation set created by automatically extracting positive and negative samples arbitrarily from the test images. Our validation set consists of 3000 positive and 6000 negative image patches.

4.2 Parameter Selection

Various filtering techniques, such as Gaussian filtering, bilateral filtering, median filtering and sharpening were tested. The results show that the sharpening technique performs better than other preprocessing steps. The size of the filters for every preprocessing technique is selected equal to 5×5 pixels. Experiments were also performed to select the optimal parameter configuration for the HOG algorithm. The parameter selection is based on the optimization of the well-known metric of F1-score that the algorithm achieves on the validation set.

Two alternative methods were tested for merging channel gradients for the HOG feature extraction procedure. Given that the terms C_{iX} and C_{iY} represent the gradients of a pixel i of a channel C of a multi-spectral image along the horizontal and vertical directions,

the first method identifies for each pixel the channel $C_{max_i} = \operatorname{argmax}_C \sqrt{C_{iX}^2 + C_{iY}^2}$ associated with the largest gradient magnitude among the channels of a multi-spectral image. Then, the gradient magnitude F_i and orientation θ_i are computed as follows:

$$F_i = \sqrt{C_{max_{iX}}^2 + C_{max_{iY}}^2} \quad (5)$$

$$\theta_i = \arctan\left(\frac{C_{max_{iY}}}{C_{max_{iX}}}\right) \quad (6)$$

A second method for merging the channel gradients, proposed in (Di Zenzo, 1986), was also evaluated. In this case, the gradient magnitude F_i and the orientation θ_i are computed as follows:

$$G_{ixy} = \sum_C C_{ix} C_{iy}, \quad x, y \in \{X, Y\} \quad (7)$$

$$\theta_i = \frac{1}{2} \arctan\left(\frac{2G_{iXY}}{G_{iXX} - G_{iYY}}\right) \quad (8)$$

$$F_i = G_{iXX} \cos^2(\theta_i) + 2G_{iXY} \cos(\theta_i) \sin(\theta_i) + G_{iYY} \sin^2(\theta_i) \quad (9)$$

If θ_i is a solution, so is $\theta_i \pm \frac{\pi}{2}$. In such cases, the orientation associated with the largest gradient magnitude F_i is used for the histogram computation. Furthermore, if $G_{iXX} = G_{iYY}$ and $G_{iXY} = 0$, θ_i cannot be computed from equation (8), so it is not used.

However, both the above alternative methods for merging channel gradients were found to be inferior to the approach used in this paper, i.e. the computation of histogram of oriented gradients for each channel of a multi-spectral image and the concatenation of all histograms in a single histogram.

Three masks for gradient computation were tested. The default mask is a simple centered mask, which can be expressed as a $[-1 \ 0 \ 1]$ mask. The other masks are the Sobel and the Scharr mask with sizes 3×3 pixels. We selected the Scharr mask as it outperforms the other gradient masks. Furthermore, both signed and unsigned gradients as well as histogram bins of size 10 and 20 degrees were tested. The conclusion is that the signed gradients and histogram bins of 10 degrees perform better.

Three block configurations were tested regarding their effect on the performance of the algorithm. The first configuration is a simple block that covers the whole image patch. The second configuration consists of 4 blocks that each covers a quarter of the area of the image patch. The third configuration consists of 5 blocks, each covering a quarter of the area of the image patch. Four blocks are placed as in the previous configuration, while the fifth lies in the middle of the image patch and overlaps with the others. Both

rectangular and circular HOG kernels were tested. A rectangular kernel is divided in four smaller rectangular cells, while a circular kernel consists of 2 radial cells with the outer cell split in 4 angular cells. Experiments show that a single block with a rectangular kernel is the optimal choice.

Experiments were also conducted to determine how normalization of the HOG descriptors affects the performance of the building detector. Block normalization using the l_1 -norm or l_2 -norm, no normalization and whole feature normalization after block normalization using the l_1 -norm or l_2 -norm were attempted. The results show that leaving the descriptors unnormalized increases the classification accuracy of the proposed algorithm.

Gamma correction, suggested in (Dalal and Triggs, 2005) for improving the performance of a human detector, was also tested. Gamma correction computes the square root of the value of each pixel as the pixel's representative value in order to compensate for distortions in the viewing process. The results discourage the use of gamma correction for the task of building detection as the maximum F1-score achieved on the validation set drops by about 1.4% when gamma correction is employed.

Finally, in order to improve the classification performance of the HOG detector, we introduced hard negatives in the training phase. Results show that the maximum F1-score on the validation set increases by 1.3% when the hard negatives are introduced. Some of the conducted experiments are presented as precision-recall curves in figure 3.

The optimal parameter configuration leads to four histograms, one for each channel of the multi-spectral image (red, green, blue, near-infrared) and each of these histograms has 144 features (4 cells \times 36 bins per cell). The total descriptor length is therefore 576.

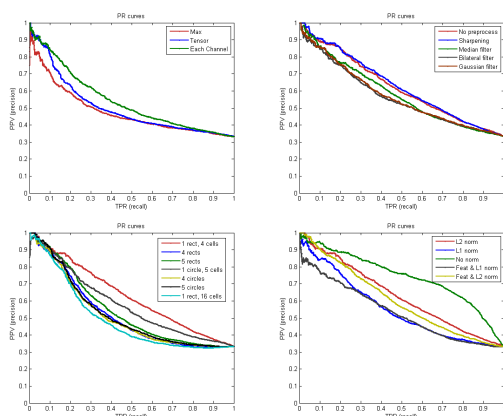


Figure 3: Precision-recall curves for HOG parameter selection.

4.3 Results

In order to detect buildings of various sizes in an image, a HOG algorithm should run in multiple scales (i.e. sizes of image regions), covering a range between a minimum and a maximum scale. The initial size in the case of a QuickBird image is 20×20 pixels and in the case of a WorldView 2 image is 22×22 pixels, given that the resolutions of the two satellites are $0.6m$ per pixel for the QuickBird and $0.5m$ per pixel for the WorldView 2 satellite. These sizes are found to be adequate to detect buildings with areas as small as $50m^2$. The displacement between two consecutive extracted image regions is equal to 5 pixels in the horizontal or the vertical direction. The ratio between two consecutive scales is selected to be equal to 1.1. The maximum image region is equal to the largest building that should be detected. In our case, such a region was selected equal to 110×110 and 130×130 pixels for the Quickbird and WorldView 2 images respectively. Such sizes can make a HOG detector capable of identifying buildings as large as approx. $3000m^2$.

After experimentation, we choose the uncertainties of the mean-shift algorithm that performs the detection merging to be equal to 3 pixels for both the x and y direction and $\log(1.3)$ for the scale. The final extracted image regions of our algorithm are checked whether they detect a building or not. A region is considered true positive if there is at least one pixel labeled as building, according to the ground truth data, in a rectangle that is located in the middle of the image region and has half the region's size. This is quite a strict rule, but we wanted to have a sufficient overlap between a region and a building to be considered true positive.

To evaluate the performance of our algorithm in the test set, we used the metrics of recall, precision and F1-score. In our context, recall is the number of detected buildings divided by the number of total buildings found in an image. Precision is defined as the number of regions that are true positives divided by the total number of the extracted image regions. Special care was taken so that buildings located at the edges of an image and are partially seen are removed. This happens because a HOG algorithm needs to enclose a sufficiently large part of a building within the extracted regions to identify it.

We run our algorithm in the 29 test images, containing 6186 buildings to evaluate the improvement from the use of the NDVI mask and the FAST features. Although the introduction of NDVI leads to a drop in the performance of our algorithm by about 1.3%, the addition of both the NDVI mask and the FAST features increases the classification accuracy of our algorithm by a measure of 4.9% with respect to

using only the HOG features. The experimental results on the test set are summarized in table 1.

Table 1: Results from the use of different features.

	Recall	Precision	F1-score
HOG	0.857	0.553	0.672
HOG+NDVI	0.858	0.54	0.663
HOG+FAST	0.825	0.613	0.704
HOG+NDVI+FAST	0.85	0.602	0.705

Finally, we would like to compare our results with two other building detection methodologies. A HOG algorithm with a different set of parameters, the most important of which are the gradient computation in the panchromatic image, the use of unsigned gradients and the block normalization using the l_1 -norm was developed in (Ilsever and Unsalan, 2013). We implemented this algorithm, but without employing the proposed shadow detection technique, in order to perform a fair comparison of the algorithms, avoiding any restrictions on the height of detected buildings.

Another building detection algorithm was developed by fusing Harris, FAST, GMSR and Gabor filtering local features (Sirmacek and Unsalan, 2011). The authors perceived these features as observations of building presence, estimated the probability density function (pdf) of these features and identified the modes this pdf as possible buildings. In this case, we consider as true positive, the case where there is at least one pixel labeled as building inside a rectangle of size 11×11 pixels around each computed building location.

The results of the different methodologies on our test set are presented in table 2. All values refer to the metric of F1-score, unless otherwise stated. The best results for each image are shown in bold. A visual comparison of the three algorithms in a part of image (area_1b,2006) of our test set is presented in figure 4.

5 CONCLUSIONS

A novel methodology for building detection was presented based on the probabilistic fusion of HOG, NDVI and FAST features. Some conclusions can be drawn by analyzing the experimental results obtained. The introduction of both NDVI and FAST features leads to better results than the use of only the HOG features. By adding these features, we manage to significantly reduce the false alarm rate of our method, while keeping the detected buildings unaffected.

Furthermore, although the training set of the HOG part of our algorithm consists of just QuickBird images, the performance of the algorithm on the World-View 2 test images is comparable to the performance

Table 2: Comparison of the algorithms on the test images.

Area \ Year		2006	2007	2009	2010	2011
area_1a	Proposed	0.645	0.701	0.64	0.681	0.665
	Ilsever	0.216	0.218	0.228	0.2	0.22
	Sirmacek	0.421	0.568	0.389	0.509	0.395
area_1b	Proposed	0.677	0.789	—	0.731	0.723
	Ilsever	0.389	0.416	—	0.392	0.399
	Sirmacek	0.509	0.506	—	0.487	0.443
area_1c	Proposed	0.757	0.791	0.819	0.823	0.804
	Ilsever	0.522	0.547	0.54	0.498	0.545
	Sirmacek	0.52	0.442	0.311	0.345	0.317
area_2a	Proposed	0.606	0.754	0.699	0.689	0.709
	Ilsever	0.277	0.322	0.309	0.282	0.276
	Sirmacek	0.526	0.59	0.376	0.166	0.075
area_2b	Proposed	0.575	0.637	0.674	0.6	0.663
	Ilsever	0.187	0.223	0.203	0.188	0.19
	Sirmacek	0.367	0.428	0.323	0.427	0.308
area_2c	Proposed	0.616	0.73	0.706	0.676	0.692
	Ilsever	0.249	0.29	0.274	0.247	0.229
	Sirmacek	0.383	0.489	0.46	0.495	0.403
Total F-score	Proposed	0.705	—	0.85	—	0.602
	Ilsever	0.303	Total Recall	0.954	Total Precision	0.18
	Sirmacek	0.416	0.286	—	0.762	—

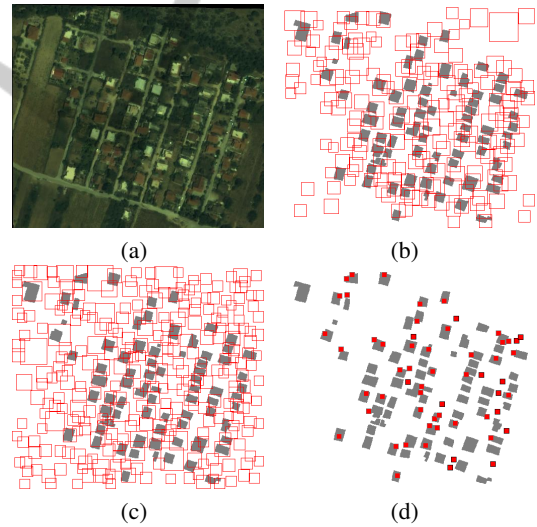


Figure 4: Detections shown in red from our method (b), (Ilsever and Unsalan, 2013)’s method (c) and (Sirmacek and Unsalan, 2011)’s method (d) overlaid on ground truth building locations of part of image (area_1b, 2006) (a).

on the QuickBird images. This fact shows that a HOG algorithm is quite robust to images taken from different satellites, making it a powerful tool for a more general satellite image processing technique.

Compared to the other algorithms, our methodology manages to significantly outperform them on all the test images with respect to the F1-score. The algorithm of Ilsever et al. identifies more buildings but the false alarm rate is too high. On the other hand,

the feature fusion of Sirmacek et al. achieves a really high precision but it cannot detect many buildings in the test set. Finally, a comparison of the two HOG implementations reveals the importance of a correct parameter configuration for the task at hand.

ACKNOWLEDGEMENTS

We would like to thank Dr. Beril Sirmacek for providing her code for our evaluation results. This research has been co-financed by the European Union (European Social Fund-ESF) and Greek national funds through the Operational Program "Education and Lifelong Learning" of the National Strategic Reference Framework (NSRF)-Research Funding Program: THALIS-NTUA-UrbanMonitor.

REFERENCES

- Benarchid, O., Raïssouni, N., Adib, S., Abbous, A., Azyat, A., Achhab, N., Lahraoua, M., and Chahboun, A. (2013). Building extraction using object-based classification and shadow information in very high resolution multispectral images, a case study: Tetuan, Morocco. *Canadian Journal on Image Processing and Computer Vision*, 4(1).
- Caselles, V., Kimmel, R., and Sapiro, G. (1995). Geodesic active contours. In *Proceedings of 5th International Conference on Computer Vision*, pages 694–699.
- Chai, D., Förstner, W., and Ying Yang, M. (2012). Combine markov random fields and marked point processes to extract building from remotely sensed images. In *ISPRS Annals of the Photogrammetry, Remote Sensing and Spatial Information Sciences*, pages 1219–1222.
- Dalal, N. (2006). *Finding People in Images and Videos*. PhD thesis, National Polytechnique de Grenoble.
- Dalal, N. and Triggs, B. (2005). Histograms of oriented gradients for human detection. In *IEEE Computer Society Conference on Computer Vision and Pattern Recognition (CVPR)*, volume 1, pages 886–893.
- Di Zenzo, S. (1986). A note on the gradient of a multi-image. *Computer Vision Graphics and Image Processing*, 33(1):116–125.
- Hallada, W. and Cox, S. (1983). Image sharpening for mixed spatial and spectral resolution satellite systems. *International Symposium on Remote Sensing of Environment*, 3:1023–1032.
- Haverkamp, D. (2004). Automatic building extraction from ikonos imagery. In *Proceedings of ASPRS*.
- Hu, J., You, S., Neumann, U., and Park, K. (2004). Building modeling from lidar and aerial imagery. In *Proceedings of ASPRS*.
- Ilsever, M. and Unsalan, C. (2013). Building detection using hog descriptors. In *6th International Conference on Recent Advances in Space Technologies (RAST)*, pages 115–119.
- Karantzalos, K. and Argialas, D. (2009). A region-based level set segmentation for automatic detection of man-made objects from aerial and satellite images. *Photogrammetric Engineering and Remote Sensing*, 75(6):667–677.
- Karantzalos, K. and Paragios, N. (2010). Large-scale building reconstruction through information fusion and 3-d priors. *IEEE Transactions on Geoscience and Remote Sensing*, 48(5):2283–2296.
- Kluckner, S. and Bischof, H. (2010). Image-based building classification and 3d modeling with super-pixels. In *Proceedings of International Society for Photogrammetry and Remote Sensing, Photogrammetric Computer Vision and Image Analysis*.
- Li, Q., Mitianoudis, N., and Stathaki, T. (2007). Spatial kernel k-harmonic means clustering for multispectral image segmentation. *Image Processing, IET*, 1(2):156–167.
- Platt, J. (1999). Probabilistic outputs for support vector machines and comparisons to regularized likelihood methods. In *Advances in Large Margin Classifiers*, pages 61–74. MIT Press.
- Rosten, E. and Drummond, T. (2006). Machine learning for high-speed corner detection. In *European Conference on Computer Vision*, pages 430–443.
- Shackelford, A. and Davis, C. (2003). A combined fuzzy pixel-based and object-based approach for classification of high-resolution multispectral data over urban areas. *IEEE Transactions on Geoscience and Remote Sensing*, 41(10):2354–2363.
- Singh, D., Maurya, R., Shukla, A., Sharma, M., and Gupta, P. R. (2012). Building extraction from very high resolution multispectral images using ndvi based segmentation and morphological operators. In *Students Conference on Engineering and Systems (SCES)*, pages 1–5.
- Sirmacek, B. and Unsalan, C. (2011). A probabilistic framework to detect buildings in aerial and satellite images. *IEEE Transactions on Geoscience and Remote Sensing*, 49(1):211–221.
- Theng, L. (2006). Automatic building extraction from satellite imagery. *Engineering Letters*, 13(3).
- Verma, V., Kumar, R., and Hsu, S. (2006). 3d building detection and modeling from aerial lidar data. In *IEEE Computer Society Conference on Computer Vision and Pattern Recognition (CVPR)*, volume 2, pages 2213–2220.
- Vinson, S., Cohen, L., and Perlant, F. (2001). Extraction of rectangular buildings in aerial images. In *Proceedings of Scandinavian Conference on Image Analysis (SCIA)*.
- Vrabel, J. (2000). Multispectral imagery advanced band sharpening study. *Photogrammetric Engineering and Remote Sensing*, 66(1):73–79.
- Woo, D., Nguyen, Q., Nguyen Tran, Q., Park, D., and Jung, Y. (2008). Building detection and reconstruction from aerial images. In *ISPRS Congress, Beijing*.